INFLUENCE OF RESIDUAL STRESS ON THE DELAMINATION AND SHEAR RESPONSE OF CARBON EPOXY COMPOSITES

S. Laik*, A. A. Skordos
Composites Centre, School of Applied Sciences, Cranfield University, MK43 0AL, UK
**suzanne.laik@insa-lyon.fr*

Keywords: Delamination, Shear, Damage, Residual stress

Abstract
The present study aims to characterise the influence of different residual stress states on mechanical and damage properties of an infusion-processed carbon fibre reinforced epoxy system. The different stress states were produced by applying various cure and post-cure profiles to the manufactured panels. The residual stresses have been evaluated using a finite element modelling solution. The in-plane shear strength and damage evolution and the mode I delamination fracture toughness have been assessed to quantify the influence of process stress. It was observed that the level of stress has a significant influence on shear strength and on delamination response. More particularly, increasing the level of stress has a positive effect on delamination strain energy release rate (increase of about 60% for an increase of 15% in residual stress) and a detrimental effect on the in-plane shear strength (decrease by approximately 20%). These results can be explained by the role of compressive stresses which resist crack opening at the delamination crack interface and accelerate fibre-matrix or matrix failure under a shear load. The influence of residual stress on the elastic response under shear including modulus evolution at a certain level of inelastic strain is negligible.

1 Introduction
Residual stresses in fibre reinforced polymer composites arise during the curing stage, due to resin shrinkage, the anisotropy in thermal expansion coefficients and the tool-part interaction [1-4]. Manufactured parts present an initial stress state that has two main effects. First, when removing a part from the mould, the combination of compressive and tensile residual stresses can result in distortion for curved geometries and non-symmetrical lay-ups [5-6]. In addtition the initial stress state has to be known accurately in order to be taken into account when considering the in-service performance of the parts.
Experimental studies have demonstrated the influence of residual stresses on mechanical properties of laminates. The different stress states have been obtained by varying the cure cycle, either by changing the dwell temperature and time [7-13], the cooling rate [10,14,15], the cooling pressure [10,14], or by applying different post-cure regimes [16]. A clear beneficial effect of residual stresses has been shown for the longitudinal tensile strength [12,16]. Transverse properties have been assessed in [13,17] by performing transverse tensile tests on UD laminates, showing an increase in transverse strength when raising the residual stresses. In cross-ply laminates, the residual stresses were also shown to enhance the properties especially the tensile strength [12]. However, the opposite result was observed in [16] where the elastic modulus decreased for higher residual stresses. It has been shown that the influence of residual stresses on the strength of cross-ply laminates was a function of the ply thickness and stacking sequence [18]. An experimental study carried out in [13] showed a weakening of the shear strength of symmetrical laminates when increasing the level of residual stresses. Residual stresses have been shown to have an influence upon the measured mode I fracture toughness of laminate composites [9,19,20]. Nairn [19] showed that ignoring the residual stresses could cause errors in the -6% to +60% range on the apparent G_{IC} value,

induced by the residual curvature strain of the DCB arms. For a doubly symmetrical laminate, there is no need to apply a correction on the experimental GIC value. An underestimation of the toughness is observed for a 0°/0° interface, which has been confirmed experimentally in [9].

Micromechanical models have been developed in order to assess the influence of residual stresses at a micro-scale. It has been showed that the presence of compressive thermal residual stresses within the matrix provides relative protection against debonds and crack propagation [17]. A realistic model considering a random fibre distribution indicated that under an inter-fibre distance of around 0.05 μm the residual stresses were no longer beneficial [21]. A beneficial effect of residual stress on transverse failure has been observed for high matrix strengths and low strength fibre-matrix interface [22, 23]. Modelling of pure shear loading confirmed the detrimental effect of residual stresses on shear strength of composite materials observed experimentally [23]. FEM studies have also been performed to study the influence of residual thermal stresses on the toughness of laminates with embedded defects for different modes of delamination [24, 25]. It has been shown that the residual stresses, in addition to an external mechanical loading, have a constraining effect on the observed mode I strain energy release rate for this kind of defects, enhancing the mode I interlaminar toughness.

The present study aims to characterise the influence of different residual stress states upon certain mechanical and damage properties of an infusion-processed carbon fibre reinforced epoxy system. The different stress states were produced by applying various postcures to the manufactured panels, after which the residual stresses have been evaluated by means of finite element modelling. The in-plane shear strength and damage evolution and the interlaminar fracture toughness, which are resin dominated properties and thus particularly affected by the presence of these residual stresses, have been assessed.

2 Experimental details

The materials used in this work were a Hexcel G1157 uniweave carbon fabric and the epoxy HexFlow® RTM6 resin. Flat plates for delamination and in-plane shear testing were manufactured. The lays-up were $[0,90,90,0,0,90,90,0,\text{insert film}]_s$ and $[\pm 45]_{2S}$, and the average thicknesses 4.3 mm and 2.2 mm respectively. For the delamination specimens, a 60 mm long, 13 μm PTFE film was used as insert for crack intiation.

The panels were produced by vacuum-assisted resin transfer moulding (VARTM) on a hot plate. The volume fibre fraction obtained was about 60%. The resin was previously degassed in a vacuum oven at 80°C. The tool was at a temperature of 120°C when the infusion started.

The cure and post-cure cycles were designed using cure kinetics modelling. A partial cure, aiming to reach a degree of cure high enough for the plates to be cut before they were subjected to the post-cure, was performed on the infusion tool. It consisted of a ramp up from 120°C to 150°C at a rate of around 1°C/min. The temperature was stabilised between 150°C and 155°C for 45 minutes, and the part was left to cool down.

The temperature was monitored using two thermocouples situated on the top and on the bottom of the part.

Four different free-standing oven postcures were performed, as follows:

1. Ramp-up at 1°C/min, dwell for 120 minutes at 180°C, slow cooling at 1°C/min, performed in the oven;
2. Ramp-up at 1°C/min, dwell for 80 minutes at 192°C, slow cooling at 1°C/min, performed in the oven;
3. Ramp-up at 1°C/min, dwell for 40 minutes at 205°C, slow cooling at 1°C/min, performed in the oven;
4. Ramp-up at 1°C/min, dwell for 40 minutes at 180°C, fast cooling at 25°C/min, performed at ambient temperature (23°C) with a fan.

In-plane-shear (IPS) testing was performed according to standard BS EN ISO 14129-1998 [26] The IPS specimens (dimensions 25 x 250 mm) were cut out from the 2.2 mm-thick plates. Aluminium tabs (dimensions 25 x 50 x 0.7 mm) were bonded with Araldite 420 on both ends of the specimens, after cleaning the area of bonding with acetone. One side of the specimens was white-painted and then speckled with black paint, creating a random pattern to monitor the strain field by 3D digital image correlation using the Limess VIC3D system. An Instron 5500R test machine, equipped with a 100kN load cell, was used for the tests, with a speed of 2 mm/min. The digital image correlation system recorded a synchronised sequence of images of the specimen, load and displacement. The first specimen of each series of tests was subjected to a monotonic IPS test, in order to obtain the envelope of the load-displacement for each batch of specimens. The rest of the specimens followed a cyclic loading profile using the maximum value of displacement obtained in the monotonic test to determine the values of cross-head displacement where the cross-head direction would be reversed. The shear modulus was obtained from the shear stress-shear strain curves. The initial modulus corresponds to the slope of the tangent to this curve, considering the first points showing no more than 1% deviation of slope from the previous points in the curve. The shear modulus for each following cycle was obtained by calculating the slope between the highest and the lowest points of the cycle.
The delamination testing was performed according to standard BS ISO 15024:2001 [27]. The delamination specimens (dimensions 20 x 200 mm) were cut from the 4.3 mm-thick plates. One edge of the specimens was marked at every millimetre for the 6 first centimetres from the end of the insert film, then every five millimetres until 130 mm. The tabs were bonded on the cracked end of the specimen. A Zwick machine equipped with a 10kN load cell was used to perform the test, at a rate of 2 mm/min. The crack was propagated over a length of 120 mm, the crack length being determined by visual observation with the aid of a magnifying lens. The load and displacement were recorded all along the test. The data analysis was performed according to the corrected beam theory described in BS ISO 15024:2001. The critical energy release rate G_{IC} was determined accounting for large displacement and load block corrections. The calculation also accounts for the exact thickness and width of the specimens, the initial length of the crack and the dimensions of the tabs. To ensure reproducibility the results were taken for values of crack length situated in a region of stable propagation. The window, determined after performing all the tests, was from 64 to 112 mm. A mean of the G_I values of re-initiation and arrest calculated within this window for each batch of specimens was calculated.

3 Modelling

The model used for the determination of cure profiles is a non-parametric cure kinetics model taken from and based on interpolation of experimental data obtained by DSC on RTM6 resin [28]. This model, given a time-temperature set of data and an initial degree of cure, calculates the reaction rate and the degree of cure of the resin throughout the cycle. The model was implemented in Excel spreadsheet and used to determine the degree of cure reached at the end of the partial cure of the parts; this value taken as the starting state for determining the degree of cure after each post-cure.
Two models were built using MSC.Marc/Mentat to determine the residual stresses development within the delamination and IPS specimens throughout each post-cure. The only difference between these two models was the number and the orientation of the plies, accounting for the stacking sequences of the specimens, $[0,90,90,0]_{2s}$ and $[\pm 45]_{2s}$ respectively. The models consist of a unit section of the specimens; each laminate layer being made of two layers of a single element. Thus the models comprise 16 elements (68 nodes) and 32 elements (132 nodes) for the IPS and the delamination specimens respectively. Two initial conditions

were applied to all the nodes of the models: the starting degree of cure and temperature at the beginning of the post-cure. While the starting degree of cure remained unchanged for the different post-cures, as the panels underwent the same curing profile before the post-cure stage, the initial temperature was modified for each post-cure. The nodes of the upper and lower faces of the models were subjected to a fixed temperature condition, which followed the different post-cure profiles. These time-temperature profiles were implemented from the beginning of the high temperature dwell, thus consisting of the dwell, the cooling stage and a final dwell at room temperature allowing the temperature to stabilise within the part at the end of the cycle. Two types of mechanical boundary conditions were used. The x, y and z translations were fixed for one corner node and the layers were forced to undergo the same strain in plane directions to represent the infinite symmetry of the geometry.

The cure shrinkage associated with the development of the degree of cure and the dependence of thermal expansion and mechanical behaviour on temperature were taken into account in the non-linear thermo-mechanical analysis. The cure kinetic equations and parameters are based on the work of Karkanas et al [29, 30] and the material models and parameters for thermal, mechanical and thermo-mechanical properties are based on published data [31, 32].

According to the non-parametric cure kinetics model used, the degree of cure reached after the partial cure of the part was 0.85. The degrees of cure obtained with the four different cure cycles are between 0.925 and 0.982. According to [3, 33] beyond a degree of cure of 0.91, the evolution of mechanical characteristics is negligible, so that the differences of degree of cure obtained in this study should not have any influence on mechanical properties. The residual stress states have been evaluated via the finite-element models. In both models, the residual stresses are found to be compressive in the direction of fibres and tensile in the transverse direction to fibres. The absolute values of tensile and compressive residual stresses are reported in Table 1. A 15% increase of the residual stresses is obtained for an increase of the dwell temperature of 25°C (from 180°C to 205°C). The cooling rate has no influence upon the level of residual stresses. This is explained by the fact that the models did not take into account the visco-elastic behaviour of the resin, and thus did not account for the phenomenon of stress relaxation that occurs during a slow cooling.

Profile	Post cure temperature (^{o}C)	Cooling rate (^{o}C/min)	Residual stress (MPa)
1	180	1	58
2	192	1	62
3	205	1	67
4	205	25	67

Table 1. Residual stress levels for the four different post cures

4 Results

The results of the IPS tests show a significant dependence on the level of residual stresses. Figure 1.a shows the stress-strain curve for three of the four post-cures, the ones where the dwell temperature has been varied, but not the cooling rate. It is observed that the residual stresses level has a negative influence not only on the level of shear strength by the specimens but also on the maximum shear strain. The shear strength and the maximum shear strain for the whole set of measurements are illustrated in Figure 1.b. The shear strength and the maximum strain decrease with the level of residual stresses. A decrease of 20% and 35% in respectively is observed for an increase of 15% in residual stresses. The cooling rate raises the shear strength and the maximum shear strain by 8% and 12% respectively.

The influence of damage level on the evolution of the shear modulus G12 throughout the cycles for the different levels of residual stresses is illustrated in Figure 7. G12 is clearly observed to decrease with the level of shear strain the specimen is subjected to. In terms of

absolute values, almost no influence is seen between the 180°C and 192°C postcures, i.e. for an increase of 7%, while the 205°C-slow cooling postcure shows values of G12 clearly lower than the previous ones. This postcure has a difference of 15% and 8% in residual stresses with the 180°C and the 192°C postcures, respectively.

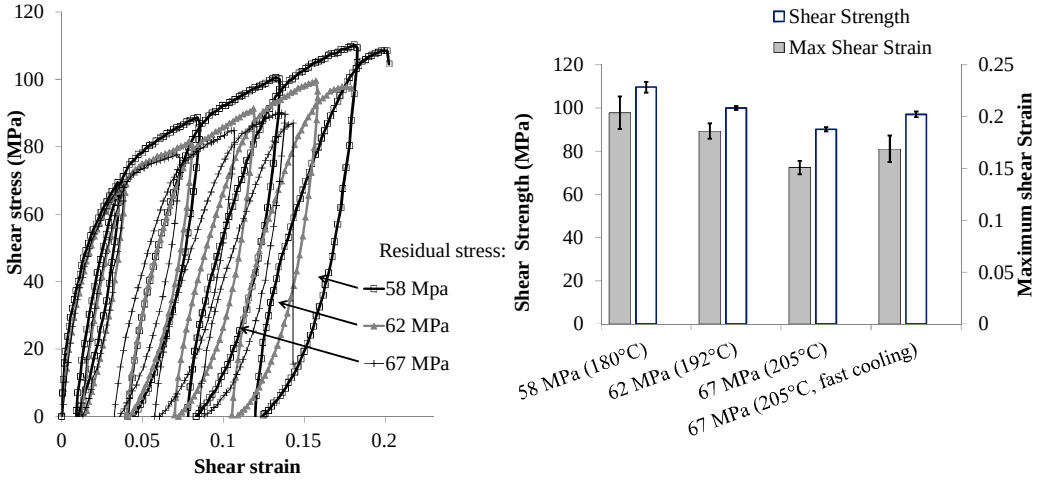

(a) (b)

Figure 1 In-plane shear behaviour as a function of residual stress: (a) Characteristic cyclic loading stress-strain curves; (b) Average shear strength and maximum strain.

Figure 2.a shows the R-curves (energy release rate in function of the length of delamination) for the four different residual stress states. The influence of residual stresses is manifested in these data. In order to compare representative values, an average of G_I for re-initiation (corresponding to the peaks in the R-curve) and arrest (the valleys) are presented in Figure 2.b. The energy release rate increases with the level of residual stresses generated by changing the dwell temperature: for an increase of the latter by 15%, $G_{I(re\text{-}initiation)}$ and $G_{I(arrest)}$ rise by 60%. The cooling rate produces the opposite effect, by reducing the values of G_I by 20%. The values of $G_{I(initiation)}$ are on average about 6% higher than of $G_{I(arrest)}$. The residual stresses do not appear to bring any changes to the $G_{I(initiation)}/G_{I(arrest)}$ ratio.

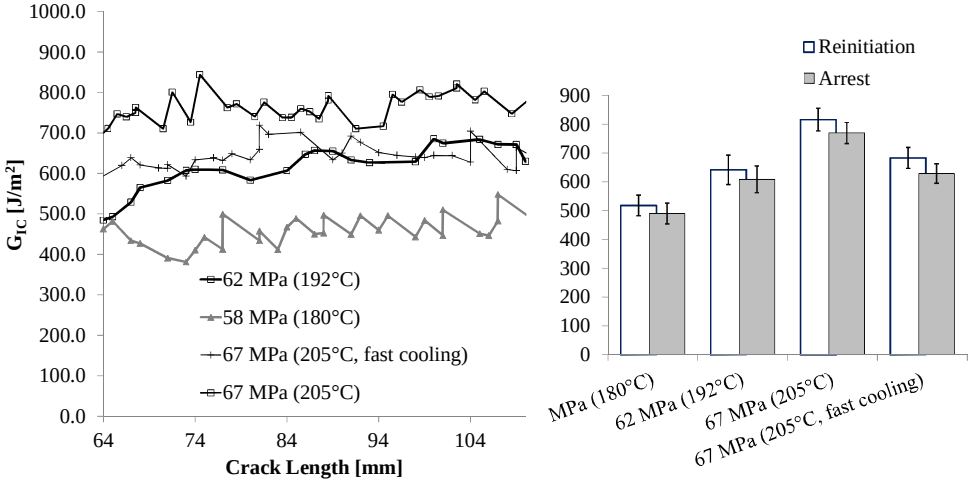

(a) (b)

Figure 2 Mode I Delamination behaviour as a function of residual stress: (a) Characteristic G_I versus crack length curves; (b) G_I (re-initiation and arrest) for different residual stress levels.

5 Discussion

The profile of stresses omputed by the models is explained by the fact that from the lamina point of view, the contraction is larger in the transverse to the fibre direction than in the longitudinal direction. The constraint each lamina is subjected to from the neighbouring layers, orientated at 90°, induces a compressive residual stress in the fibre direction and a tensile residual stress, equal in absolute value, in the transverse direction. Significant consequences are induced in terms of mechanical properties.

Increasing the residual stresses results in decreasing the shear strength and the shear strain to failure of the IPS specimens. The external tensile load applied during the tests gives a maximum shear stress at an angle of ±45° with respect to the specimen direction. The residual stresses in these directions are either tensile (in the transverse direction to the fibres) or compressive (in the direction of the fibres). Although the compressive residual stresses tend to delay the failure of the plies, the transverse tensile residual stresses act the opposite by adding to the external tensile shear stress. Thus, the level of residual tensile stresses in the transverse direction to fibres within each ply is critical for the overall failure of the specimens. Therefore, the higher the residual stresses are the earlier the failure occurs.

The results of mode I delamination showed that increasing the level of residual stress enhanced the delamination resistance of the $[0,90,90,0,0,90,90,0,crack]_s$ specimens. As highlighted in Nairn's work [19], in doubly-symmetric laminates the residual stresses do not cause any initial curvature of the beams. Thus, the layers at the centre of the specimens, orientated 0°, play the most important role in the toughness as the crack propagates between them. The increase of compressive residual stresses within these layers could be the cause of an increased delamination toughness. Compressive stresses could compete with the mode I tensile load applied to the specimen. Moreover, a fibre-bridging phenomenon has been observed in samples subjected to higher residual stresses states (indicating that the crack propagation has been partially blocked and possibly deviated at times during the test.

6 Conclusions

The influence of residual stresses on mechanical properties of composites produced by infusion has been investigated in this study. It has been shown that a 15% increase in residual stresses could change the toughness and the shear strength up to about 60% and 20% respectively. This effect was positive on delamination properties, but negative on shear properties. This proves the importance of accounting for even small levels of residual stresses, as they can bring significant changes in mechanical performances, either in a bad or good way. These results indicate that although residual stress is generally considered as a defict, there could design situations in which its presence could be considered beneficial.

Acknowledgment

Financial support from the FP7 project Infucomp is gratefully acknowledged.

References

[1] Wisnom M, Gigliotti M, Ersoy N, Campbell M, Potter K. Mechanisms generating residual stresses and distortion during manufacture of polymer–matrix composite structures. Composites Part A: Applied Science and Manufacturing Apr. 2006; 37(4):522-529.

[2] Ersoy N et al. Development of the properties of a carbon fibre reinforced thermosetting composite through cure. Composites Part A: Applied Science and Manufacturing Mar. 2010; 41(3):401-409.

[3] White SR and Hahn HT. Process modeling of composite materials: residual stress development during cure. Part II. Experimental validation. Journal of Composite Materials 1992; 26(16):2423.
[4] Taylor P, Antonucci V, Giordano M, Nasser J, Nicolais L. Process-Induced Residual Stresses in Polymer-Based Composites. Polymer News 2005, 30(8): 238-247.
[5] Cowley K. The measurement and prediction of residual stresses in carbon-fibre/polymer composites. Composites science and technology 1997; 57(11):1445-1455.
[6] Kim KS, Hahn HT. Residual stress development during processing of graphite/epoxy composite. Composites Science and Technology 1989; 36(2):121-132.
[7] Bogetti TA, Gillespie JW. Process-Induced Stress and Deformation in Thick-Section Thermoset Composite Laminates. Journal of Composite Materials 1992; 26(5):626-660.
[8] Kim YK. Cure cycle effect on composite structures manufactured by resin transfer molding. Journal of composite materials 2002; 36(14): 1725, 2002.
[9] Olivier PA, Tarsha-Kurdi KE. Process-induced stresses and their influence upon some mechqnicql properties of carbon/epoxy laminates. Part I : mode I delamination behavior of carbon /epoxy laminates. Study of 0 ° / 0 ° and ± 45 °. Proceedings of ECCM-11 Conference. Rhodes (Greece), May, 2004.
[10] White S, Hahn H. Cure cycle optimization for the reduction of processing-induced residual stresses in composite materials. Journal of composite materials 1993; 27(14): 1352-1378.
[11] Gopal A. Optimal temperature profiles for minimum residual stress in the cure process of polymer composites. Composite Structures 2000; 48(1-3): 99-106.
[12] Kurdi-Tarsha KE, Olivier PA. Assessment of the effects of process-induced stresses on some mechanical properties of carbon/epoxy laminates by acoustic emission. Proceedings of ICCM-14 Conference, San Diego (USA), June, 2003.
[13] Olivier PA, Sawi I. Designing curing conditions in order to analyse the influence of process-induced stresses upon some mechanical properties of carbon / epoxy laminates at constant Tg and degree of cure. International Journal of Material Forming 2010; 3(2):1373-1389.
[14] Tarsha-Kurdi KE, Olivier P. Thermoviscoelastic analysis of residual curing stresses and the influence of autoclave pressure on these stresses in carbon/epoxy laminates. Composites Science and Technology 2002; 62(4):559-565.
[15] Sicot O, Gong XL, Cherouat A, Lu J. Determination of Residual Stress in Composite Laminates Using the Incremental Hole-drilling Method. Journal of Composite Materials 2003; 37(9): 831-844.
[16] Sicot O, Gong XL, Cherouat A, Lu J. Influence of residual stresses on the mechanical behavior of composite laminate materials. Advanced Composite Materials 2005; 14(4): 319-342.
[17] Correa E, Mantič V, París F. Effect of thermal residual stresses on matrix failure under transverse tension at micromechanical level: A numerical and experimental analysis. Composites Science and Technology 2011; 71(5): 622-629.
[18] Flaggs DL. Experimental Determination of the In Situ Transverse Lamina Strength in Graphite/Epoxy Laminates. Journal of Composite Materials 1982; 16(2):103-116.
[19] Nairn JA. Energy release rate analysis for adhesive and laminate double cantilever beam specimens emphasizing the effect of residual stresses. International Journal of Adhesion and Adhesives 200; 20(1):59-70.
[20] Nairn JA. Fracture mechanics of composites with residual thermal stresses. Journal of Applied Mechanics 1997; 64: 804–810.
[21] Maligno AR, Warrior NA, Long AC. Effects of inter-fibre spacing on damage evolution in unidirectional (UD) fibre-reinforced composites. European Journal of Mechanics - A/Solids 2009; 28(4):768-776.
[22] Ishikawa T. Strengths and thermal residual stresses of unidirectional composites. Journal of Composite Materials 1982; 16(1):40.
[23] Zhao L, Warrior N, and Long A. A micromechanical study of residual stress and its effect on transverse failure in polymer–matrix composites. International Journal of Solids and Structures 2006; 43(18-19):5449-5467.

[24] Pradhan B, Panda S. The influence of ply sequence and thermoelastic stress field on asymmetric delamination crack growth behavior of embedded elliptical delaminations in laminated FRP composites. Composites Science and Technology 2006; 66(3-4): 417-426.
[25] Babu P, Pradhan B. Effect of damage levels and curing stresses on delamination growth behaviour emanating from circular holes in laminated FRP composites. Composites Part A: Applied Science and Manufacturing 2007; 38(12):2412-2421.
[26] BSI. Fibre-reinforced plastic composites - Determination of the stress / shear strain response, including the in-plane shear modulus and strength by the ± 45 ° tension test method. 1998.
[27] BSI. Fibre-reinforced plastic composites - Determination of mode I interlaminar fracture toughness , G IC , for unidirectionally reinforced materials. 2001.
[28] Skordos AA, Partridge IK. Cure kinetics modelling of epoxy resins using a non-parametric numerical procedure. Polymer Engineering and Science 2001; 41: 793-805.
[29] Karkanas PI, Partridge IK. Cure modeling and monitoring of epoxy/amine resin systems. I. Cure kinetics modeling. Journal of Applied Polymer Science 2000; 77(7):1419-1431.
[30] Karkanas PI, Partridge IK. Cure modeling and monitoring of epoxy/amine resin systems. II. Network formation and chemoviscosity modeling. Journal of Applied Polymer Science 2000; 77(10): 2178-2188.
[31] Skordos AA, Partridge IK. Inverse heat transfer for optimization and on-line thermal properties estimation in composites curing. Inverse Problems In Science And Engineering 2004; 12:157-172.
[32] Svanberg JM. Prediction of Shape Distortions for a Curved Composite C-spar. Journal of Reinforced Plastics and Composites 2005; 24(3): 323-339.
[33] White SR, Hahn, HT. Mechanical property and residual stress development during cure of a graphite/BMI composite. Polymer Engineering & Science 1990; 22:1548-2634.